



Universiteit
Leiden
The Netherlands

Growing LaAlO₃/SrTiO₃ interfaces by sputter deposition

Dildar, I.M.; Neklyudova, M.; Xu, Q.; Zandbergen, H.W.; Harkema, S.; Boltje, D.B.; Aarts, J.

Citation

Dildar, I. M., Neklyudova, M., Xu, Q., Zandbergen, H. W., Harkema, S., Boltje, D. B., & Aarts, J. (2015). Growing LaAlO₃/SrTiO₃ interfaces by sputter deposition. *Aip Advances*, 2015(5), 067156. doi:10.1063/1.4923285

Version: Not Applicable (or Unknown)

License: [Leiden University Non-exclusive license](#)

Downloaded from: <https://hdl.handle.net/1887/45077>

Note: To cite this publication please use the final published version (if applicable).



Growing LaAlO₃/SrTiO₃ interfaces by sputter deposition

I. M. Dildar, M. Neklyudova, Q. Xu, H. W. Zandbergen, S. Harkema, D. Boltje, and J. Aarts

Citation: *AIP Advances* **5**, 067156 (2015); doi: 10.1063/1.4923285

View online: <http://dx.doi.org/10.1063/1.4923285>

View Table of Contents: <http://scitation.aip.org/content/aip/journal/adva/5/6?ver=pdfcov>

Published by the *AIP Publishing*

Articles you may be interested in

[Epitaxial strain and its relaxation at the LaAlO₃/SrTiO₃ interface](#)

J. Appl. Phys. **120**, 085302 (2016); 10.1063/1.4961330

[Role of the interface on radiation damage in the SrTiO₃/LaAlO₃ heterostructure under Ne²⁺ ion irradiation](#)

J. Appl. Phys. **115**, 124315 (2014); 10.1063/1.4870052

[Creation of a two-dimensional electron gas and conductivity switching of nanowires at the LaAlO₃/SrTiO₃ interface grown by 90° off-axis sputtering](#)

Appl. Phys. Lett. **103**, 071604 (2013); 10.1063/1.4817921

[Stoichiometry of LaAlO₃ films grown on SrTiO₃ by pulsed laser deposition](#)

J. Appl. Phys. **114**, 027008 (2013); 10.1063/1.4811821

[Non-conducting interfaces of LaAlO₃/SrTiO₃ produced in sputter deposition: The role of stoichiometry](#)

Appl. Phys. Lett. **102**, 121601 (2013); 10.1063/1.4798828

The advertisement features a blue and orange background with a molecular structure graphic. On the left is a thumbnail of an 'Applied Physics Reviews' journal cover. The main text reads 'NEW Special Topic Sections' in large white font. Below this, it says 'NOW ONLINE' in orange, followed by 'Lithium Niobate Properties and Applications: Reviews of Emerging Trends' in white. The AIP Applied Physics Reviews logo is in the bottom right corner.

NEW Special Topic Sections

NOW ONLINE
Lithium Niobate Properties and Applications:
Reviews of Emerging Trends

AIP Applied Physics Reviews

Growing LaAlO₃/SrTiO₃ interfaces by sputter deposition

I. M. Dildar,^{1,a} M. Neklyudova,² Q. Xu,² H. W. Zandbergen,² S. Harkema,³
D. Boltje,⁴ and J. Aarts^{4,b}

¹Kamerlingh Onnes Laboratorium, Leiden University, The Netherlands

²National Center for High Resolution Microscopy, Kavli Institute for Nanoscience, Delft Technical University, Lorentzweg 1, 2628 CJ Delft, The Netherlands

³Faculty of Science and Technology and MESA+ Institute for Nanotechnology, University of Twente, 7500 AE Enschede, The Netherlands

⁴Huygens - Kamerlingh Onnes Laboratorium, Leiden University, The Netherlands

(Received 30 December 2014; accepted 15 June 2015; published online 26 June 2015)

Sputter deposition of oxide materials in a high-pressure oxygen atmosphere is a well-known technique to produce thin films of perovskite oxides in particular. Also interfaces can be fabricated, which we demonstrated recently by growing LaAlO₃ on SrTiO₃ substrates and showing that the interface showed the same high degree of epitaxy and atomic order as is made by pulsed laser deposition. However, the high pressure sputtering of oxides is not trivial and number of parameters are needed to be optimized for epitaxial growth. Here we elaborate on the earlier work to show that only a relatively small parameter window exists with respect to oxygen pressure, growth temperature, radiofrequency power supply and target to substrate distance. In particular the sensitivity to oxygen pressure makes it more difficult to vary the oxygen stoichiometry at the interface, yielding it insulating rather than conducting. © 2015 Author(s). All article content, except where otherwise noted, is licensed under a Creative Commons Attribution 3.0 Unported License. [<http://dx.doi.org/10.1063/1.4923285>]

I. INTRODUCTION

Ever since the pioneering work by Ohtomo & Hwang¹ in 2004 there has been interest in studying the properties of the interface between band insulators such as LaAlO₃ (LAO) and SrTiO₃ (STO), which yield conducting interfaces and a two-dimensional electron gas. Most of the work is done using the technique of pulsed laser deposition (PLD) and by now it is clear that the occurrence of conductance is a complicated interplay between self-doping of the interface to avoid divergence of the electric potential, the production of oxygen defects in the deposition process, and the stoichiometry of the growing film.² Conductance requires a TiO₂-terminated STO surface to furnish the correct surface charge state as well as the required Ti 3*d* orbitals^{1,3} and a critical thickness of 4 unit cells of LAO.⁴ When grown by PLD, different conductivity regimes are found for different amount of background oxygen pressure;⁵⁻⁷ around 10⁻⁶ mbar the conducting layer extends into the STO bulk, interface conductance is found around 10⁻³ mbar, and insulating interfaces are produced above 10⁻² mbar.^{8,9} One facet of the problem which only recently entered the discussion is the importance of the stoichiometry of the LAO layer, more in particular the La:Al ratio. In a study using molecular beam epitaxy (MBE) as growth technique, it was shown that interfaces can be tuned from conducting to insulating by varying the La and Al ratio in the films,^{10,11} with conducting interfaces forming only for a ratio slightly below 1. Subsequently it was shown that for the non-conducting interfaces grown by sputtering in high pressure oxygen the ratio was about 1.1.^{12,13} Similar results were reported for PLD-grown samples,¹⁴ and also a relation was established between stoichiometry and laser fluence.¹⁵⁻¹⁷ It should further be mentioned that conducting interfaces could be grown by

^aPresent address: University of Engineering and Technology, Lahore, Pakistan

^bElectronic mail: aarts@physics.leidenuniv.nl



high pressure sputtering in pure argon using an off-axis geometry,¹⁸ which presumably led to the desired stoichiometry. Here we report in more detail on radiofrequency (RF) sputter deposition of LaAlO₃ on SrTiO₃ in an on-axis geometry and using a high oxygen pressure. The interfaces can be made sharp and coherent, but were found to be non-conducting and the LAO films La-rich.^{12,13} It may be thought that varying the oxygen pressure can lead to different results and conducting interfaces. We show the outcome of the growth process under different parameters and the effects of post annealing treatments. In particular with respect to temperature and oxygen pressure we find a growth window for depositing smooth and crystalline films, which appears to preclude the correct stoichiometry for obtaining interface conductance. Using a La-poor target did not make a difference, nor did the use of argon as sputter gas instead of oxygen.

II. EXPERIMENT

We performed sputter deposition of LaAlO₃ on SrTiO₃ at oxygen pressure between 0.28 mbar and 1.2 mbar and substrate temperatures between 800 °C and 1000 °C in an on-axis growth mode using an RF power source. The high pressure avoids back-sputtering and damage in the growing thin films.¹⁹ The best results with respect to epitaxy, roughness, and sharp interfaces were obtained with a stoichiometric target at an oxygen pressure of 0.8 mbar and a substrate temperature of 920 °C.

Target and substrates

Non-conducting LaAlO₃ (LAO) targets made of pressed powder with nominal composition of La₁Al₁O₃ (designated as stoichiometric) and (La_{0.94}Al_{1.06}O₃ (called non-stoichiometric) were purchased from commercial companies with a purity of 99.9%, and a density better than 96%. SrTiO₃ (STO) with (001) orientation was used as substrate. It has a lattice constant of (3.905 Å), implying a mismatch with LAO ($a_c = 3.79$ Å) films which leads to compressive strain in the film of about 2 %. TiO₂-terminated SrTiO₃ surfaces were obtained after thermal and chemical treatment^{20,21} to control the growth on atomic scale. In this paper, only TiO₂-terminated surfaces are used, which were provided by TSST B.V, Enschede, the Netherlands.

Thin film growth process

Substrates with sizes varying from 5 mm × 5 mm to 10 mm × 10 mm were glued on a heater with a conducting silver paste which remains conducting at high temperatures and has a melting point of 960°C. A number of used STO substrates are glued around the substrate on which the film is to be deposited to ensure the homogeneity of the temperature. The substrate and side plates are pre-baked at 300°C in air to make the glue harder in order to sustain high temperatures. A heater cover with a hole of 1.5 cm is used to have only substrates and side plates face the plasma, which helps to avoid contamination of the whole heater. The system is pumped down with a turbo pump for typically 8 hours which achieves a pressure of 1×10^{-7} mbar. Oxygen with 5N purity is entered into the system monitored by a flow meter. The pressure is regulated with the rotation speed of the turbo pump, controlled by software. In RF sputtering, 20 W power was always used for pre-sputtering the target and 30 W or higher for deposition. The heater is mounted on a on an arm which can be rotated over different targets, and the chosen deposition temperature is set before it is rotated into position above a target which is already ignited. After deposition, the samples were cooled down in vacuum. It takes about 5 hours to cool down to room temperature. Some samples of LaAlO₃ were cooled down in the growth pressure of oxygen but no significant changes were observed in the properties of those films.

Film characterization techniques

Atomic force microscopy was used to inspect the topography of all the grown LAO films. To investigate the quality of the films, we used x-ray diffraction (XRD). X-ray reflectometry (XRR) was

used to determine thickness, density, and roughness of thin films. For some samples high resolution two-dimensional Reciprocal Space micrograph (RSM) measurements were performed with a Bruker D8 discoverer, equipped with a monochromator ($\lambda = 1.5406 \text{ \AA}$) and a Vantec-1 array detector at Twente University. X-ray photo-electron spectroscopy (XPS) was used to determine the surface stoichiometry of some films. Interfaces were investigated by high-resolution transmission electron microscopy (HR-TEM), energy dispersive x-ray (TEM/EDX) and electron energy loss spectroscopy (EELS).

III. SPUTTER GROWN LAO/STO FILMS AND INTERFACES

Crystal growth, being a non-equilibrium kinetic process, depends (in the case of sputter deposition) on a number of parameters such as deposition temperature T_{dp} , process gas pressure P_{dp} , target-to-substrate distance, energy of the deposited particles, etc. First we concentrate on determining a window for (T_{dp}, P_{dp}) to obtain smooth and epitaxial growth. A number of films was grown from the stoichiometric target on TiO_2 -terminated STO substrates at a given forward power and target-to-sample distance. Each film was given an identifier (LAxx) in order to facilitate comparison. For the first set of films the distance between target and substrate was about 4 cm, and the RF forward power was 30 W. We determined the surface roughness by AFM and the out-of-plane lattice constant c_o since epitaxial film should be under strain, which is then reflected in (a smaller value of) c_0 . The interpretation is somewhat more complicated, however, since the value of c_0 is not only influenced by the strain in the film, but also by the stoichiometry, as will be discussed later. Before giving more details, the main results are collected in Table I. They show for instance that the growth rate depends on pressure as might be expected, but also increases with increasing temperature. There is a narrow window of small roughness around 920 °C- 940 °C and 0.8 mbar. Growing outside this window results in rough and structurally defective films. More trends are visible in Table I. At 1.2 mbar, smooth films can be grown, but that requires very high temperature. Films grown at 0.6 mbar are smooth, but they have larger lattice constants than bulk LAO, which indicates the films do not consist of coherently strained LaAlO_3 . At 0.4 mbar, films are smooth but no LAO film peak can be seen in diffraction experiments. The lowest growth pressure used to grow LAO films is 0.28 mbar. The surface is then very rough and, as we will see, backsputtering impedes the growth of LAO film.

Some films were cooled down in the growth pressure of 0.8 mbar, but no significant change in morphology, lattice constant, XPS elemental spectra and conductivity was observed. For the

TABLE I. Sputter deposition parameters of LaAlO_3 on SrTiO_3 . Given are the sputter gas pressure P_{dp} , the substrate temperature T_{dp} , the roughness of the LAO film as measured by AFM, the out-of-plane lattice constant c_o , the LAO film thickness, the growth time t_{dp} (in minutes), the deposition rate R_{dp} and the sample identifier. The forward power used to grow these films is 30 W.

P_{dp} (mbar)	T_{dp} (°C)	Rough. (nm)	c_o (Å)	d_{LAO} (nm)	t_{dp} (min)	R_{dp} (nm/min)	Sample ID
2	800	1.6	<i>see text</i>				
1.2	800	1.6	x	5	120	0.04	LA44
1.2	840	1.7	x	15	306	0.05	LA37
1.2	900	2.1	x	8	60	0.13	LA48
1.2	1034	0.2	3.786	13	120	0.11	LA47
1.0	840	1.4	3.789	13	160	0.08	LA38
0.8	840	2	3.789	13	120	0.11	LA36
0.8	920	0.2	3.786	20	120	0.17	LA51
0.8	920	0.4	3.777	12	90	0.13	LA69
0.8	940	0.2	3.766	12	90	0.13	LA72
0.6	940	0.8	3.799	14	100	0.14	LA68
0.4	940	0.2	x	15	60	0.25	LA67
0.28	840	22	x	x	30	x	LA9

TABLE II. Effect of forward power on LAO films grown at $T_{dp} = 920^\circ\text{C}$ and $P_{dp} = 0.8$ mbar. Given are the forward (FW) power, the roughness of the LAO film, the out-of-plane lattice constant c_o , the LAO film thickness, rate of deposition R_{dp} , growth time t_{dp} and relative identity (ID) for each sample.

Power (W)	Rough. (nm)	c_o (Å)	d_{LAO} (nm)	R_{dp} (nm/min)	t_{dp} (min)	Sample ID
30	0.1	3.786	21	0.16	120	LA53
40	0.2	3.788	32	0.27	120	LA54
50	0.4	3.773	35	0.3	120	LA55
60	0.4	3.799	51	0.43	120	LA56
70	0.2	3.808	x	x	60	LA57
80	0.2	3.817	x	x	60	LA58
90	0.3	3.813	x	x	60	LA59

optimized values at 30 W, $P_{dp} = 0.8$ mbar, $T_{dp} = 920^\circ\text{C}$, the growth rate is 0.17 nm/min. We decreased the target to substrate distance to 2 cm in order to increase the growth rate. This did not change the quality of the films.

We also investigated the effects of changing the forward power for growth in the window ($T_{dp} = 920^\circ\text{C}$ and $P_{dp} = 0.8$ mbar). As can be seen in the Table II, increasing the forward power from 30 W first increases the roughness, while above 60 W the value of c_o started to increase, again reaching values above the bulk lattice parameter of LAO. Note that to compensate for the increase of sputter rate with power, we halved the growth time above 60 W. Apparently, both a lower sputter gas pressure and high RF power leads to more energy being deposited during growth, and a change in the film composition. In the next two paragraphs we give more details on the AFM and XRD results.

A. Surface characterization by AFM

We discussed in the previous section that the sputtering allows a small temperature and pressure window to work in, based on AFM surface roughness measurements. Below we give several examples. AFM software was used for the image rendering, data smoothing, height profiles and roughness analysis using a standard area of $1\mu\text{m}$.

Figure 1 shows the results of some films grown at 2 mbar of oxygen at different temperatures. The growth time is 15 minutes for all, while the forward power is 70 W (LA1, LA3) or 75 W (LA2).

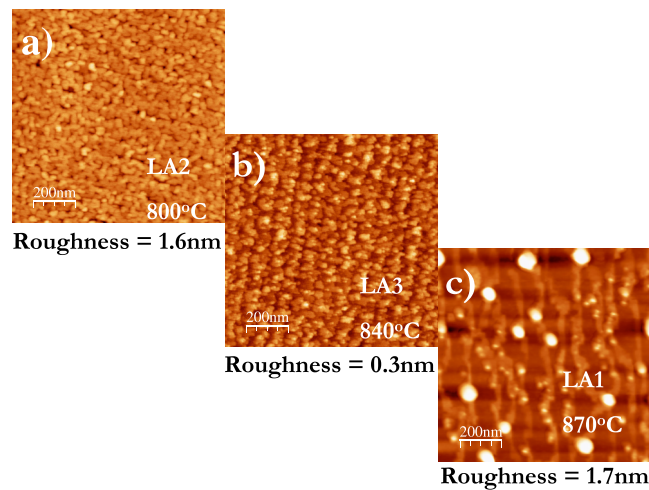


FIG. 1. Surface morphology of LAO film grown at 2 mbar of oxygen pressure for 15 minutes at different growth temperatures (a) LA2 grown at 800°C (b) LA3 grown at 840°C (c) LA1 grown at 870°C .

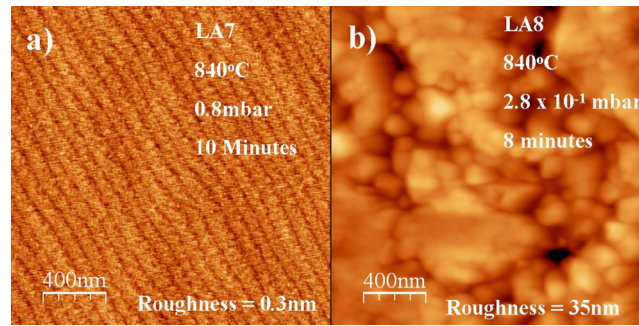


FIG. 2. Surface morphology of LAO films grown at 840°C for approximately the same time at different growth pressures. (a) LA7 grown at 0.8 mbar of oxygen pressure (b) LA8 grown at 0.28 mbar of oxygen pressure.

The change in temperature has a clear effect on the morphology. The film grown at 800°C shows grains and the roughness is high (1.6 nm). The film grown at 840°C has decorated steps. The film is very smooth (0.3 nm). The film grown at 870°C is rough again (1.7 nm) and shows some outgrowths along with irregular terraces.

We observe that LA3 grown at 840°C looks better in morphology than the other two films. The next step was to reduce the pressure but keep the temperature at 840°C. The resulting films with the corresponding morphological changes are shown in figure 2. The film at 0.8 mbar shows nicely spaced steps while the film at 0.28 mbar has larger grains forming like clusters and is very rough (35 nm). Varying the temperature at the growth pressure of 0.8 mbar yields smooth films (0.3 nm) at 920°C. Figure 3 shows the surface morphology of a 20 nm film (LA51). The corresponding profile (Figure 3(b)) indicates a roughness of 0.2 nm, indicating a mixed LaO /AlO₂ termination, although that could not be resolved.

To see the effects of the high temperature growth and the cooling procedure on the TiO₂-terminated surface of the STO substrate, some substrates were passed through all deposition steps without depositing a LaAlO₃ film. The surface morphology of the substrates before and after heating is shown in figure 4. They were heated up to 920°C at 0.8 mbar of oxygen pressure, remained at that temperature for 10 minutes and were then cooled down to room temperature in two different ways. The sample shown in figure 4(a) was cooled down in vacuum and the sample shown in figure 4(c) was cooled down in oxygen pressure of 0.8 mbar. There is no appreciable change in morphology measured by AFM before and after heating, although the terrace structure in the oxygen-cooled down sample is somewhat better preserved. Since this comes closer to the growth conditions (the low vacuum can cause additional oxygen loss from the substrate), we conclude that the starting surface for growth is unchanged by the high temperature.

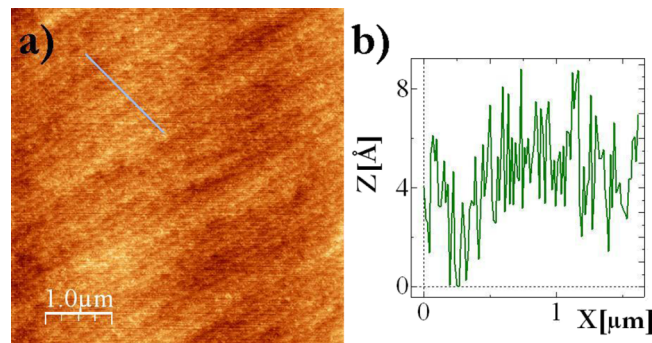


FIG. 3. Surface morphology of a 20 nm thin film of LAO grown at optimized growth parameters, 920°C, 0.8 mbar of oxygen pressure and 30 W power. (a) topography (b) height profile of (a).

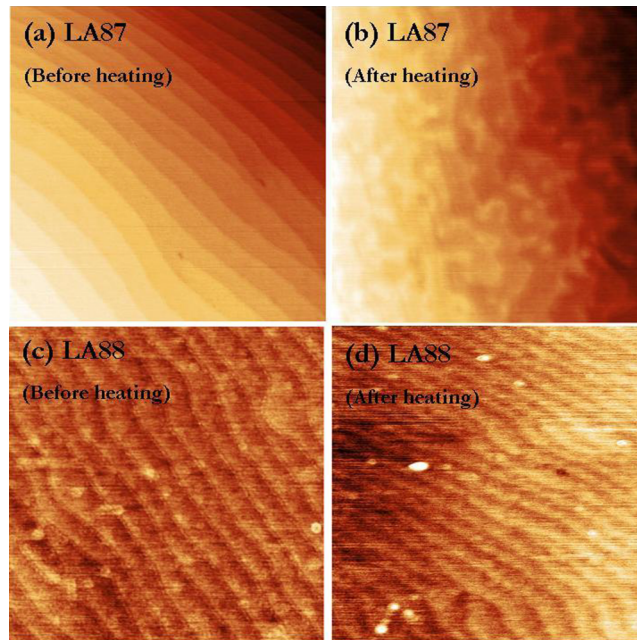


FIG. 4. Annealing effects on surface morphology of a $\text{SrTiO}_3\text{-TiO}_2$ terminated surface (a,c) The STO surface before annealing; (b,d) the same substrates after heating to 920°C followed by (b) cooling in vacuum (LA87), (d) cooling in 0.8 mbar of oxygen (LA88).

B. Characterization by XPS

In the early stage of finding the growth window, x-ray photoelectron spectroscopy was used. Figure 5 shows spectra of two LAO films grown at 2 mbar and 0.28 mbar of pressure at a temperature of 840°C . A wide range of binding energies is measured to obtain information about the elements present at the surface. Figure 5(a) shows peaks of La and Al and also small peaks of Sr and Ti while in figure 5(b), almost only Sr is visible. We conclude from this that at 0.28 mbar, back-sputtering is strong enough to prevent film deposition.

C. Thickness and Structure of LaAlO_3 thin films by XRD

In our earlier work¹³ we showed the change in lattice parameter c_0 for films of different thickness grown at optimal conditions, to illustrate the effect of relaxation. Here we are more concerned with the overall effect of different growth parameters on the quality of the deposited LAO. In Figure 6 we show XRD data on films with roughly the same thickness (14 nm, 12 nm, 15 nm), grown at (940°C , 0.6 mbar; film LA68), (920°C , 0.8 mbar), (910°C , 0.8 mbar), (940°C , 0.8 mbar) and from the non-stoichiometric target at (940°C , 0.8 mbar). The values should be compared to the bulk lattice constant of LAO ($a_o = 3.789 \text{ \AA}$) and show that LA68 and the film from the non-stoichiometric target have a larger lattice parameter than the bulk, opposite to what can be expected from strain. We come back to this in the discussion.

D. Structure of LaAlO_3 thin films by RSM

Reciprocal space mapping gives extra information about the epitaxy of the thin films. In Figure 7, three films are shown. The film on the left (LA109, thickness 16 nm) and right (LA116, thickness 8 nm) are grown with pressure (0.8 mbar) and RF power (30 W), and temperature 920°C and 850°C , respectively, LA56 (middle panel) was grown at a forward power of 60 W. The reflection for LA109 and LA56 are taken around (123) and for LA116 around (103). Lattice parameters (in-plane c_{in} , out-of-plane c_0) calculated from these maps are given in Table III. Film LA56, grown

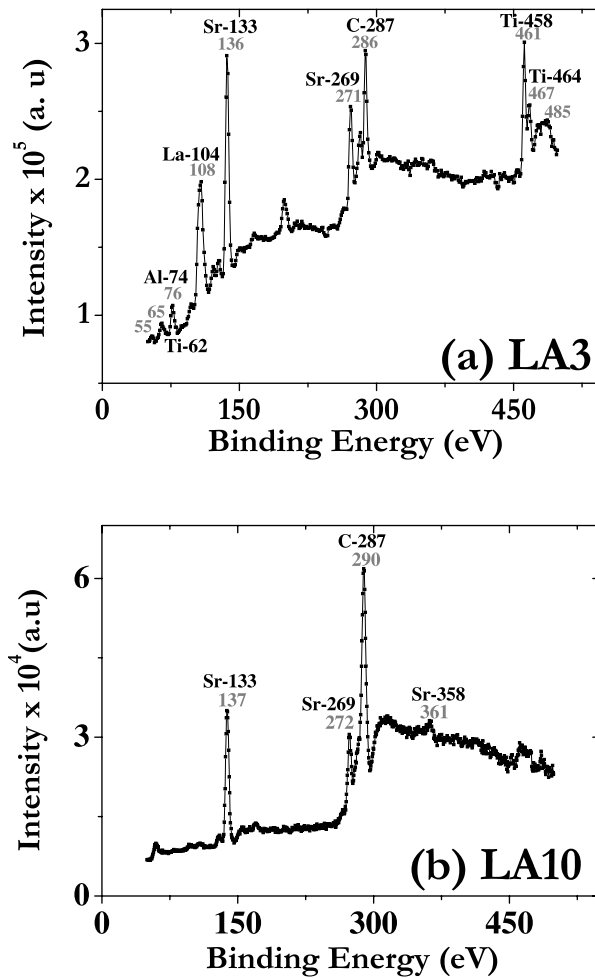


FIG. 5. An X-ray photoelectron spectroscopy of two LAO films on STO. (Top) grown at 2 mbar and 840 °C, shows the peaks of La and Al with strong peak of Sr and small peaks of Ti, (Bottom) grown at 0.28 mbar and 840 °C shows diffusion of Sr at the surface of LAO film.

at a higher power (60 W) than optimized, does not have an epitaxial relation with the substrate, as can be seen from the in-plane lattice parameter. The volume of cell is also calculated as it has a direct relation with the La/Al ratio.²² This will be discussed in detail later.

IV. THE LAO/STO INTERFACE

We already reported on the determination of the stoichiometry of the LAO films by using TEM with energy dispersive x-ray detection (TEM / EDX), from which we found a La / Al ratio of 1.07 for films deposited under optimal conditions. Below we show TEM pictures of various samples.

A. Quality and sharpness of interface

As we demonstrated above, sputtering allows a small window for crystalline films. Figure 8 shows the TEM image of two films of LAO on STO, LA37 and LA47, which were grown at $P_{dp} = 1.2$ mbar and $T_{dp} = 840^\circ\text{C}$ and 1034°C respectively (see Table I). For LA37 small and discontinuous patches can be seen as shown in figure 8(upper). The film shown in Figure 8(lower) (LA47) looks more smooth, both at the surface and at the interface, in agreement with the AFM

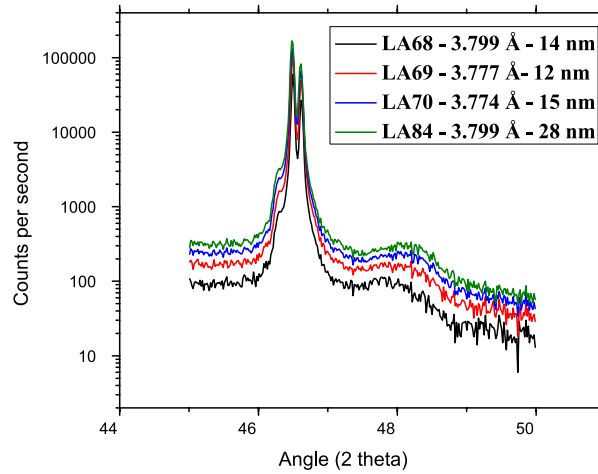


FIG. 6. XRD data of some representatives films of LAO at angles around the STO(002) reflection, which corresponds to a lattice parameter of 3.904 Å. The baseline of all data sets coincided, and for clarity the three upper sets have been vertically shifted with respect to the lowest set (black line). From bottom to top: LA68, 14 nm, grown at 940 °C and 0.6 mbar (black line); LA69, 12 nm, grown at 920 °C and 0.8 mbar (red line); LA70, 15 nm, grown at 910 °C and 0.8 mbar (blue line); LA84, 28 nm, grown at 940 °C and 0.8 mbar (green line). LA84 was grown with a non-stoichiometric target.

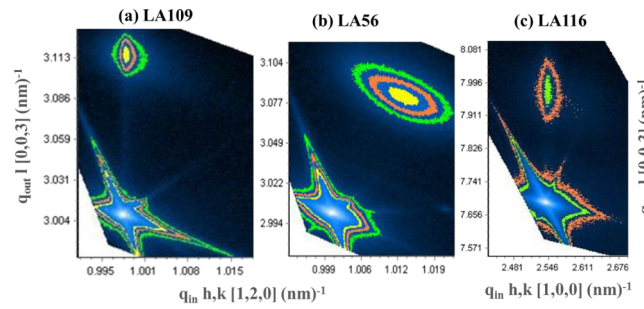


FIG. 7. Reciprocal space maps for (a) LA109 (16 nm) and (b) LA56 (51 nm) taken around the (123) direction; (c) LA116 (8 nm) taken around the (103) direction.

TABLE III. Comparison of out-of-plane (c_o) and in-plane (c_{in}) lattice parameters of LAO films under different growth conditions. Also given are the power, the growth temperature T_{dp} and the volume. The fully strained films are grown at the optimized parameters, $T_{dp} = 920^\circ\text{C}$, $P_{dp} = 0.8$ mbar and power = 30 W. The relaxed films are grown either at higher forward power (60 W; LA56) or at lower temperature 850°C; LA108). LA56 and LA51 can also be found in Table II, Table I, respectively. The cell volume is also given as it has a relation with the La/Al ratio.²²

Sample ID	Power W	T_{dp} °C	c_o (Å)	c_{in} (Å)	Volume (Å) ³	Remarks
LA56	60	920	3.792	3.852	56.26	relaxed
LA109	30	850	3.788	3.847	56.06	relaxed
LA108	30	920	3.770	3.906	57.52	strained
LA116	30	920	3.764	3.906	57.43	strained
LA51	30	920	3.786	3.906	57.76	strained

results, but there are small etch pits. In these cases, it cannot be ruled out that the insulating behavior which was found for these films is the result of their discontinuous nature.

For a good comparison, Figure 9 shows the already published TEM micrograph of an atomically sharp LAO/STO interface, made on film LA51, which is itself homogeneous and smooth.

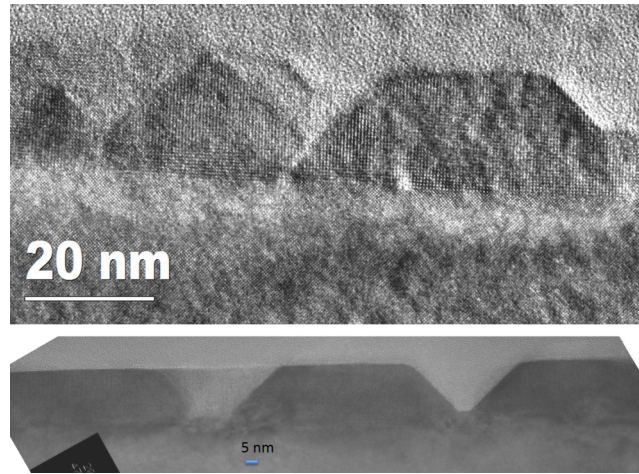


FIG. 8. TEM micrographs of two films of LAO on STO. Upper: LA37, grown at 840°C, 1.2 mbar; lower: LA47, grown at 1034°C, 1.2 mbar.

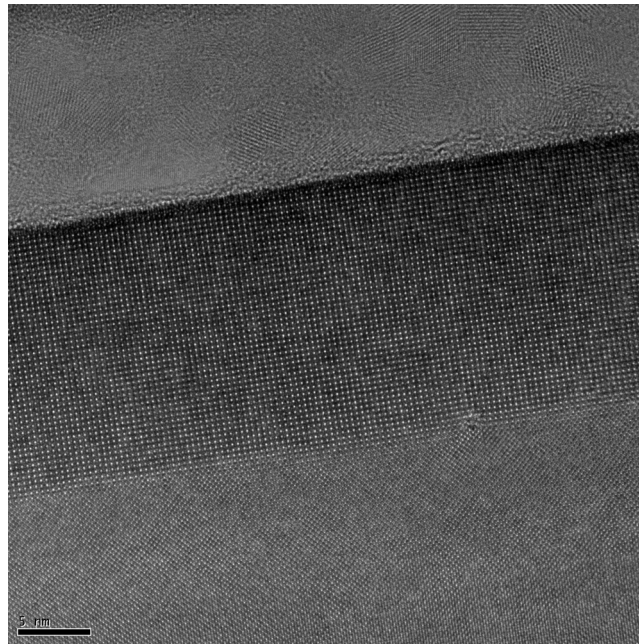


FIG. 9. High resolution TEM picture of the LAO/STO interface for film LA51 grown on optimized growth parameters, at 920 °C and 0.8 mbar.

B. Attempts to fabricate conducting interfaces

The conductance of a number of films grown under optimal growth conditions was measured at room temperature and at 10 K. We used bonded wires in a 4-point measurement, with contacts in line. Typical values of the resistance were 10M Ω and above where 10 k Ω to 100 k Ω could be expected. The high oxygen pressure possibly prevents the formation of oxygen defects and can compensate the deficiency of oxygen. It should be kept in mind that in PLD grown conducting interfaces, crystallinity is not an essential requirement. Amorphous films of LAO at 10⁻³ mbar can also make the interface conducting.²³ With this idea, we varied the growth parameters beyond the optimized growth window ($T_{dp} = 920^{\circ}\text{C}$ and $P_{dp} = 0.8$ mbar). We changed the oxygen flow, introduced argon gas and also a mixture of argon and oxygen (50,50) but the interfaces were not conducting. Also reducing the pressure below the optimized pressure (table I) can produce amorphous films but the

interface still remains non-conducting. Applying an electric field to these non-conducting interfaces to tune the interfacial conductance did not change the insulating behavior either.

We also used a non-stoichiometric LaAlO_3 target ($\text{La} = 0.94, \text{Al} = 1.06$) to enhance the elemental contribution of Al in the grown films. There is no appreciable change in morphology, surface roughness by AFM, or lattice constant of these films. Their stoichiometry measured by TEM/EDX gives the ratio $\text{La}/\text{Al} = 1.06$ (LA78), not significantly different from the result from the stoichiometric target. We also tried to put extra Al in the film by gluing pieces of sapphire (Al_2O_3) on the La-defective target. Clear changes were seen in morphology, with a rougher surface but conduction was not induced. It appears that the high-pressure oxygen environment inhibits strong changes in the La/Al ratio of the film.

V. DISCUSSION

The LAO films grown at the (high) oxygen pressure of 0.8 mbar and a temperature of 920 °C are found to be smooth and the structure is crystalline. The interfaces are sharp, with intermixing of a few unit cells as also seen in PLD- or MBE-grown samples, and insulating. They closely resemble the high pressure PLD grown interfaces reported on by Kalabukhov *et al.*⁸ which are also insulating. This points to the important role of oxygen vacancies in conducting interfaces grown by PLD. Both in high-pressure PLD and in high-pressure sputtering, it appears that the amount of oxygen vacancies produced in the growth process becomes too low to generate a doped interface. This is probably both a consequence of the quenching of the vacancy production by highly energetic particles in the PLD- or sputter-plasma and the larger amount of oxygen available to refill the formed vacancy.

The optimal temperature for sputtered grown films is significantly higher than used for PLD grown films (typical temperature range 750°C- 850 °C). This may have consequences for the atomic structure of the starting surface. On the one hand we showed that, by taking STO substrates through the deposition steps without growing, the surface of such a substrate has not changed significantly. On the other hand, it is conceivable that the starting surface at the growth conditions is different at the higher temperature and pressure.²⁴ Still, it is more probable that the chemical processes of the growth are influenced by the high temperature. It is interesting to note that the conducting interfaces produced by 90° off-axis sputtering¹⁸ were also prepared at the lower temperature. Moreover, they were grown in Argon instead of Oxygen, which we did not find possible in our on-axis geometry. It is interesting to speculate that this mode of sputtering produces enough oxygen to grow the film, without saturating vacancies which are formed in the process.

This information can be combined with the knowledge on stoichiometry. From TEM/EDX data we earlier found a La/Al ratio of the optimally grown films of about 1.06, which is above the critical ratio of 0.97 for conductance determined by Warusawithana *et al.* Ref. 11. We also showed this to be in agreement with the values of the out-of-plane lattice parameter, which not only is lower than the bulk lattice parameter of LAO due to the strain, but also varies considerably as function of the La/Al ratio²² with $c_0 \approx 0.3764$ nm for a ratio of 1, but ≈ 0.378 nm when $\text{La}/\text{Al} = 1.1$. Looking at Tables I-III we see that the typical values are around 0.378 nm, except for LA116, grown at 850 °C (Table III) where $c_0 = 0.3764$. Those films, however, were not very smooth. The value for c_0 reported for the off-axis deposition in Ref. 22 is 0.374 nm, which would correspond to a ratio $\text{La}/\text{Al} = 0.9$ and therefore in the conducting regime. It is interesting to note that the off-axis deposition was performed at a pressure of 0.2 mbar, which suggests that the off-stoichiometry is due to the increased scattering of the light Al atoms in the higher pressure, although it still cannot be ruled out that the higher substrate temperature plays a role. With respect to the consequences of a ratio La/Al larger or smaller than 1, this was investigated theoretically by Hellberg,²⁵ using first-principle DFT calculations. He concluded that in La-rich films, Al vacancies are formed rather than that La is substituted for Al. These vacancies can migrate to the interface and screen the polar discontinuity, so that the metallic interface does not form. On the experimental side, it can be speculated that the stoichiometry also has a bearing on the effects of post-annealing. The results of Cancellieri *et al.*⁹ show that the interface conductance of samples grown at 10⁴ mbar can be changed

by postannealing, suggesting that the basic stoichiometry allows conductance, but that the amount of oxygen vacancies still can be varied. On the other hand, once the film has been grown with a stoichiometry which does not allow conductance, postannealing does not change that. It appears therefore that the pressure-temperature window to grow epitaxial films of LAO on STO required by the on-axis geometry precludes control over the stoichiometry of the film.

VI. CONCLUSION

In conclusion, we have grown LAO/STO interfaces by sputtering in high oxygen pressure in an on-axis geometry. We find a relatively small window in substrate temperature and sputter gas pressure where smooth films are grown with atomically sharp interfaces. The films show an excess of La, while the interfaces are not conducting; nor can they be rendered conducting by a post-anneal treatment. The sputter geometry does not allow to find a set of conditions which would lead to a deficit of La, which is needed to render the interface conducting.

ACKNOWLEDGEMENTS

We would like to thank M. B. S. Hesselberth for technical assistance and advice. The research was funded in part through a research grant from the Foundation for Fundamental Research on Matter (FOM), which is part of the Netherlands Organization for Scientific Research (NWO). I. M. D. was supported by the Higher Education Commission (HEC) of Pakistan and on study leave from the Department of Physics, University of Engineering and Technology (UET), Lahore, Pakistan. M.N., Q.X. and H.W.Z. gratefully acknowledge ERC project 267922 for support.

- ¹ A. Ohtomo and H. Hwang, *Nature* **427**, 423 (2004).
- ² N. C. Bristowe, P. Ghosez, P. B. Littlewood, and E. Artacho, *J. Phys. Cond. Matt.* **26**, 143201 (2014).
- ³ N. Nakagawa, H. Y. Hwang, and D. A. Muller, *Nature Materials* **5**, 204 (2006).
- ⁴ S. Thiel, G. Hammert, A. Schmehl, C. W. Schneider, and J. Mannhart, *Science* **313**, 1942 (2006).
- ⁵ A. Kalabukhov, R. Gunnarsson, J. Borjesson, E. Olsson, T. Claeson, and D. Winkler, *Phys. Rev. B* **75**, 121404(R) (2007).
- ⁶ A. Brinkman, M. Huijben, M. v. Zalk, J. Huijben, U. Zeitler, J. C. Maan, G. v. d. Wiel, G. Rijnders, D. H. A. Blank, and H. Hilgenkamp, *Nature Mat.* **6**, 493 (2007).
- ⁷ M. Huijben, A. Brinkman, G. Koster, G. Rijnders, H. Hilgenkamp, and D. H. A. Blank, *Adv. Mat.* **21**, 1665 (2009).
- ⁸ A. Kalabukhov, Y. A. Boikov, I. T. Serenkov, V. I. Sakharov, J. Borjesson, N. Ljustine, E. Olsson, D. Winkler, and T. Claeson, *Europhys. Lett.* **93**, 37001 (2011).
- ⁹ C. Cancellieri, N. Reyren, S. Gariglio, A. D. Caviglia, and J.-M. Triscone, *Europhys. Lett.* **91**, 17004 (2010).
- ¹⁰ M. P. Warusawithana, A. A. Pawlicki, T. Heeg, D. G. Schlom, C. Richter, S. Paetel, J. MANNHART, M. Zheng, B. Mulcahy, J. N. Eckstein, W. Zander, and J. Schubert, *Bulletin of the APS* **55**(2), (2010), abstract ID BAPS.2010.MAR.B37.1.
- ¹¹ M. P. Warusawithana, C. Richter, J. A. Mundy, P. Roy, J. Ludwig, S. Paetel, T. Heeg, A. A. Pawlicki, L. F. Kourkoutis, M. Zheng, M. Lee, B. Mulcahy, W. Zander, Y. Zhu, J. Schubert, J. N. Eckstein, D. A. Muller, C. S. Hellberg, J. Mannhart, and D. G. Schlom, *Nat. Comm.* **4**, 2351 (2013).
- ¹² I. M. Dildar, D. Boltje, M. Hesselberth, J. Aarts, Q. Xu, H. W. Zandbergen, and S. Harkema, *e-JSSNT* **10**, 1 (2012).
- ¹³ I. M. Dildar, D. B. Boltje, M. H. S. Hesselberth, J. Aarts, Q. Xu, H. W. Zandbergen, and S. Harkema, *Appl. Phys. Lett.* **102**, 121601 (2013).
- ¹⁴ E. Breckenfeld, N. Bronn, J. Karthik, A. R. Damodaran, S. Lee, N. Mason, and L. W. Martin, *Phys. Rev. Lett.* **110**, 196804 (2013).
- ¹⁵ T. C. Droubay, L. Qiao, T. C. Kaspar, M. H. Engelhard, V. Shutthanandan, and S. A. Chambers, *Appl. Phys. Lett.* **97**, 124105 (2010).
- ¹⁶ S. Wicklein, A. Sambri, S. Amoruso, X. Wang, R. Bruzzese, A. Koehl, and R. Dittmann, *Appl. Phys. Lett.* **101**, 131601 (2012).
- ¹⁷ H. K. Sato, C. Bell, Y. Hikita, and H. Y. Hwang, *Appl. Phys. Lett.* **102**, 251602 (2013).
- ¹⁸ J. P. Podkaminer, T. Hernandez, M. Huang, S. Ryu, C. W. Bark, S. H. Baek, J. C. Frederick, T. H. Kim, K. H. Cho, J. Levy, M. S. Rzchowski, and C. B. Eom, *Appl. Phys. Lett.* **103**, 071604 (2013).
- ¹⁹ X. X. Xi, G. Linjer, O. meyer, E. Nold, B. Obst, F. Radzel, R. Smithy, B. Strehlau, F. Weschenfelder, and J. Geerk, *Zeitsch. Physik B* **74**, 13 (1989).
- ²⁰ M. Kawasaki, K. Takahashi, T. Maeda, R. Tsuchiya, M. Shinohara, O. Ishiyama, T. Yonezawa, M. Yoshimoto, and H. Koinuma, *Science* **266**, 1540 (1994).
- ²¹ G. Koster, B. L. Kropman, G. J. H. M. Rijnders, D. H. A. Blank, and H. Rogalla, *Appl. Phys. Lett.* **73**, 2920 (1998).
- ²² L. Qiao, T. C. Droubay, T. Varga, M. E. Bowden, V. Shutthanandan, Z. Zhu, T. C. Kaspar, and S. A. Chambers, *Phys. Rev. B* **83**, 085408 (2011).
- ²³ Y. Z. Chen, D. V. Christensen, F. Trier, N. Pryds, A. Smith, and S. Linderroth, *Appl. Surf. Science* **258**, 9242 (2012).
- ²⁴ M. B. S. Hesselberth, S. J. van der Molen, and J. Aarts, *Appl. Phys. Lett.* **104**, 051609 (2014).
- ²⁵ C. S. Hellberg, *Bulletin of the APS* **56**(1), (2011), abstract ID BAPS.2011.MAR.A34.5.